arXiv:cond-mat/9710309v1 [cond-mat.mes-hall] 29 Oct 1997

Charge and current oscillations in Fractional quantum Hall systems with edges

J. Shiraishi[1*], Y.Avishai[1,2†] and M. Kohmoto[1‡]

[1] *Institute for Solid State Physics, University of Tokyo Roppongi, Minato-ku, Tokyo 106 Japan*

[2] *Physics Department, Ben Gurion University of the Negev, Beer Sheva, Israel*

(June 15, 2017)

Abstract

Stationary solutions of the Chern-Simons effective field theory for the fractional quantum Hall systems with edges are presented for Hall bar, disk and annulus. In the infinitely long Hall bar geometry (non compact case), the charge density is shown to be monotonic inside the sample. In sharp contrast, spatial oscillatory modes of charge density are found for the two circular geometries, which indicate that in systems with compact geometry, charge and current exist also far from the edges.

*e-mail address: shiraish@ginnan.issp.u-tokyo.ac.jp

†e-mail address: yshai@bgumail.bgu.ac.il

‡e-mail address: kohmoto@issp.u-tokyo.ac.jp

I. INTRODUCTION

The present work focuses on charge and current distributions in clean two dimensional electronic systems with edges which are subject to strong perpendicular magnetic fields. Investigating the physics of the integer or fractional quantum Hall effect (QHE), and in particular, elucidation of the precise charge and current profiles in these systems is a fundamental problem from both theoretical and practical experimental points of view. The quantum mechanical dynamics of electrons in two dimensional systems at strong magnetic field is characterized by two fundamental concepts. The first one is the formation of Landau levels which play an essential role in the studies of integer QHE. The second, and probably more profound is the effect of the Coulomb interaction and the emergence of the fractional QHE.

Indeed, a substantial theoretical effort has been devoted to compute the charge and current distributions within a realistic quantum mechanical picture. For the integer QHE in an infinitely long Hall bar, a self consistent formalism relating charge density and electrostatic potential has been suggested [1]. Numerical solutions of the pertinent equations indicate that the charge density is monotonic decreasing inside the Hall bar, and has a power law singularity ($|x-L|^{-1/2}$) at the edges [1]. In the particular geometry of a semi-infinite plan, an analytic solution using the Wiener-Hopf method is obtained [2], and the charge density is found to have the same power law singularity near the single edge.

For two dimensional electronic systems at very strong magnetic fields the electron-electron interaction plays a fundamental role, as it leads to the fractional quantum Hall effect (and in fact, according to the global picture [3], also to the integer quantum Hall effect). Hence, an evaluation of the charge and current profiles in the fractional QHE is somewhat more intricate. One of the successful methods for describing the fractional QHE is the effective Chern-Simons gauge field theory [4], which includes the Coulomb interaction in a non-perturbative manner. Employing this theory for the calculations of charge and current distributions is therefore distinct from various other approximations used for treat-

ing these quantities in interacting systems. These include Hartree [5], Hartree-Fock [6] and others [7].

In the present work, calculation of charge and current profiles are based on the Chern-Simons field theory for treating the fractional quantum Hall liquids. It turns out however, that in order to preserve gauge invariance, inclusion of edges within this formalism must be done carefully. One possible approach [8] is to add a one dimensional edge term to the original action. (See also [9,10] and refs. therein.) Once it is assumed that all the important physical quantities are concentrated near the edges, this chiral edge action becomes a powerful tool for studying the various edge effects. Thereby, the theory is formulated through the Tomonaga-Luttinger liquid description, whose experimental verification is under intense investigation especially in tunneling experiments. Recently, such tunneling effects were measured and found to be consistent with theoretical predictions [11].

While studying the physics pertaining to stationary quantum Hall states in which there are 'non-zero' currents flowing, one has no apriori knowledge of whether or not charge and current are concentrated near the edge. In order to approach this problem, we start our investigation from the Chern-Simons effective theory which treats edge and bulk properties on an equal footing [12]. It leads, among other results, to a set of self-consistent equations for charge and current distributions within the two-dimensional sample. In the most general case, for filling factor $\nu = m/(mp+1)$ with integer m and even p, there are $3m \times 3m$ coupled integro-differential equations. Here we restrict ourself to stationary solutions with $m = 1$ (non-hierarchial case). For clean systems with sufficiently high symmetry it ends up with a single homogeneous eigenvalue problem determined by an integro-differential equation. This equation was derived in ref. [12] for the Hall bar geometry, and appears to be markedly different from its anlalogous one for the integer QHE [1].

One of the interesting problems is to study the spectrum of the eigenvalue equation thus obtained. For the integer QHE, it is suggested that the spectrum is continuous [1]. On the other hand, nothing is known for the fractional case so far. If we assume that the spectrum is continuous also for the fractional case, the integro-differential equations can be solved

analytically order by order and it leads to a charge distribution which is finite at the edges [13].

We present below a general method for solving the pertinent equations both for the integer [1] and the fractional [12] QHE systems. Unlike the previous order by order treatment, our method is based on the Green function method for solving eigenvalue problems. The general method is then applied for some specific systems of physical interest.

Our results indicate that for the infinitely long Hall bar geometry, only a single eigenvalue exists, which is physically acceptable, and the corresponding charge distribution agrees with the one obtained earlier using the analytic method [13]. For the disk and annulus geometries, many physically acceptable eigenvalues are present, and the corresponding solutions behave as radial modes $\rho_n(r)$ with n nodes between R_1 and R_2. This surprising appearance of spatial charge oscillations in fractional quantum Hall systems with compact geometries has not been noticed before, and might shed a new light on the physics of edge channels.

In Section 2, we explain the Green function method which is used in solving the equations for the charge density. For convenience, the method is explained within the Hall bar geometry. The solutions for the charge and current profiles in a disk and an annulus, which comprise the novel part of the present work are presented in Section 3. A few specific topics are discussed in the Appendices. In Appendix A, the Green function method for the integer QHE system [1] is discussed, while in Appendix B, the results for the fractional QHE in the Hall bar geometry are presented and shown to be consistent with those obtained within an analytic treatment [13]. Finally, in Appendix C, the Green function method is combined with a power expansion technique which proves to be useful for the Hall bar geometry.

II. THE GREEN FUNCTION SOLUTION

Consider an infinitely long Hall bar stretched along the y axis between the points $x = L_1$ and $x = L_2$ subject to a strong magnetic field H in the z direction. In the stationary QHE the charge density ρ depends only on x, and at present we are interested in the density profile

$\rho(x)$ for non-hierarchial filling fraction $\nu = 1/(p+1)$ with p even. Here ρ is the difference between the charge distribution and its average. The equations derived in Ref. [12] couple the charge density $\rho(x)$ and the current density $J_y(x)$, but if the later is eliminated, a single integro-differential equation for $\rho(x)$ remains, which reads

$$(8\pi\nu c g^{-1})^2 \frac{d^2}{dx^2}\rho(x) - \rho(x) = (4\nu^2 \xi g^{-1}) \frac{d^2}{dx^2} \int_{L1}^{L_2} log|x - x'|\rho(x')dx'. \tag{1}$$

In this equation c is the velocity of the Chern-Simons gauge field and g^{-1} is the coupling constant of the Maxwell term in the Chern-Simons Lagrangian. The constant $\xi \geq 0$ comes from the solution of the Poisson equation relating the electrostatic potential to the charge density. Eq.(1) must also be accompanied by the condition

$$\int_{L_1}^{L_2} \rho(x)dx = 0. \tag{2}$$

It is useful to define $q \equiv (8\pi\nu c g^{-1})^{-1}$ and scale coordinates $x \to qx$ so that the integration limits are $X_i = qL_i$. Eq.(1) then reads,

$$\frac{d^2}{dx^2}\rho(x) - \rho(x) = \mu \frac{d^2}{dx^2} \int_{X_1}^{X_2} log|x - x'|\rho(x')dx', \tag{3}$$

where all the quantities appearing in the above equation are dimensionless, including the constant $\mu \equiv \nu\xi/2\pi c$.

Before proceeding with the solution of Eq.(3) three general remarks are useful at this point. 1) Eq.(3) (and similar equations which are obtained later for other geometries) is a peculiar eigenvalue problem for the charge density ρ, which can formally be written as

$$A\rho + \mu B\rho = 0, \tag{4}$$

where A and B are certain linear operators and μ is an eigenvalue. In Eq.(4), the operator A is self adjoint but B is not. However, physics requires the existence of real eigenvalues. We show below that Eq.(3) can indeed be cast into an equation having the same form as Eq.(4) in which A is symmetric and B is symmetric and positive definite. This problem has then only real eigenvalues. 2) The value of μ appearing therein cannot be chosen arbitrarily, but

must be selected from the relevant set of eigenvalues. On the other hand, following Eq.(3), the constant μ is composed of certain physical quantities such as mass, charge, dielectric constant, filling factor *etc.* If the spectrum is discrete, it might be tempting to formulate here a kind of quantization rule. This is of course too ambitious, since the basic theory is not an exact one. On the other hand, the *sign* of μ should be consistent with its physical content. 3) It is not useful to perform the second derivative on the right hand side of Eq.(3) and obtain an integral equation. Indeed, the resulting equation will have a very singular kernel which turn its solution practically impossible. Instead, we use the Green function method which is so successful in solving eigenvalue problems of the Sturm-Lioville type.

Without loss of generality we can set the Hall bar symmetrically between the points $X_1 = -qL$ and $X_2 = qL$ (namely, $L_2 = -L_1 = L$). Furthermore, following Refs. [1,13] we limit our set of solutions to be antisymmetric, $\rho(-x) = -\rho(x)$ which automatically satisfy the condition (2). The coordinate x is then limited within the interval $[0, qL]$ and the equation for the charge density becomes,

$$\frac{d^2}{dx^2}\rho(x) - \rho(x) = \mu \frac{d^2}{dx^2} \int_0^{qL} \log \left| \frac{x - x'}{x + x'} \right| \rho(x') dx', \tag{5}$$

together with the condition $\rho(0) = 0$. The value of $\rho(qL)$ is not specified.
We look for a (symmetric) Green function $G(x, x') = G(x', x)$ which, formally can be considered as the inverse of the operator $[\frac{d^2}{dx^2} - 1]$ with the appropriate boundary conditions. Hence, it should satisfy

$$\left[\frac{d^2}{dx^2} - 1 \right] G(x, x') = \delta(x - x'), \tag{6}$$

$$G(0, x') = 0. \tag{7}$$

Denoting respectively by $x_<$ and $x_>$ the smaller and larger values of x and x', it is easily verified that

$$G(x, x') = -\sinh(x_<)\cosh(x_>) + \alpha \sinh(x)\sinh(x'), \tag{8}$$

where the second term on the right hand side reflects the freedom resulting from the absence of a second boundary condition at $x = qL$.

We now express ρ on the left hand side of Eq.(5) in terms of $G(x,x')$. Formally we apply the operator $G=[\frac{d^2}{dx^2}-1]^{-1}$ on both side of (5) and use the formal identity

$$\left[\frac{d^2}{dx^2}-1\right]^{-1}\frac{d^2}{dx^2}=1+\left[\frac{d^2}{dx^2}-1\right]^{-1}. \tag{9}$$

Strictly speaking, the operator $[\frac{d^2}{dx^2}-1]$ has a zero eigenvalue corresponding to the function $\sinh x$ so that its inverse must be defined within the subspace that is orthogonal to this function. In so doing we might abandon some of the solutions of the original equation (5). We will see however that the set of solutions is rich enough to capture the main physical content. With this point kept in mind the integro-differential equation (5) is transformed into an integral equation,

$$\rho(x)=\mu\int_0^{qL}dx'\ \log\left|\frac{x-x'}{x+x'}\right|\rho(x')+\mu\int_0^{qL}dx''\int_0^{qL}dx'\ G(x,x'')\log\left|\frac{x''-x'}{x''+x'}\right|\rho(x'). \tag{10}$$

Note that the right hand side of Eq.(10) vanishes at $x=0$ as required. The kernel of the integral equation does not appear to be symmetric, so, apriori, there is no guarantee that the eigenvalues μ are real. In order to proceed and actually show it, it is convenient to write Eq.(10) in its operator form,

$$\rho=\mu(1+G)L\rho, \tag{11}$$

where the integral operators have their obvious coordinate representations $\langle x|G|x'\rangle = G(x,x')$, $\langle x|L|x'\rangle=\log\left|\frac{x-x'}{x+x'}\right|$ (not to be confused with the system length) and $\langle x|1|x'\rangle=\delta(x-x')$, all of them are symmetric. It is not difficult to show that the operator $-L$ is positive definite, and therefore its square root $(-L)^{1/2}$ exists. Eq.(11) is then equivalent to the following equation for $\eta\equiv(-L)^{1/2}\rho$,

$$\eta=\mu(-L)^{1/2}[-(1+G)](-L)^{1/2}\eta, \tag{12}$$

whose kernel is symmetric. Only solutions corresponding to positive eigenvalues μ are physically acceptable. As we have commented after Eq.(9), every solution of Eq.(12) is also a solution of Eq.(5), but the converse is not necessarily true. Numerical solutions of Eq. (12) will be discussed in appendix B.

III. OSCILLATING CHARGE AND CURRENT DISTRIBUTION IN DISK AND ANNULUS

We now use the Green function method introduced above to solve the equations of Ref. [12] in a circular geometry and demonstrate the occurrence of spatial charge oscillations. The algorithm is demonstrated for a disk geometry, and then, later on, some minor modifications are introduced in order to study the annulus geometry. We believe that for both systems our results are experimentally relevant.

Consider a clean disk of radius R subject to a strong perpendicular magnetic field such that the filling factor is $\nu = 1/(p+1)$ with p an even number. For systems with axial symmetry the charge density ρ, the electrostatic potential V and the (tangential) current density J_θ depend only on the radial coordinate r. There is of course no radial current. It is useful to define the radial differential operator $D_r^2 \equiv \frac{d^2}{dr^2} + \frac{1}{r}\frac{d}{dr}$. Then, we obtain the following set of equations,

$$\rho(r) - \frac{1}{q^2} D_r^2 \rho(r) = \frac{4\nu^2}{g} D_r^2 V(r) \tag{13}$$

$$V(r) = -\xi \int_0^R \phi(r, r') \rho(r') r' dr' \tag{14}$$

$$\phi(r, r') = \int_0^{2\pi} \frac{d\theta}{\sqrt{r^2 + r'^2 - 2rr'\cos\theta}}, \tag{15}$$

where $q \equiv (8\pi\nu c g^{-1})^{-1}$. Of course, the last two equations are just the solution of the Poisson equation expressing the electrostatic potential $V(r)$ in terms of the charge density $\rho(r)$ for systems with axial symmetry, with $\xi \geq 0$. The charge density and the electrostatic potential are expected to be finite in the disk. In particular they should be regular at the origin. The weak singularity of $\phi(r, r')$ at $r = r'$ is then integrable.

Eliminating $V(r)$ from Eqs.(13) and transforming to dimensionless coordinates $x = qr$ we get a single integro-differential equation for $\rho(x)$,

$$[D_x^2 - 1]\rho(x) = \mu D_x^2 \int_0^{qR} \phi(x, x') \rho(x') x' dx', \tag{16}$$

where $\mu \equiv \nu\xi/2\pi c > 0$.

We look for a (symmetric) Green function $G(x,x') = G(x',x)$ which, formally can be considered as the inverse of the operator $[D_x^2 - 1]$ with the appropriate boundary conditions (regularity at $x = 0$). Hence, it should satisfy

$$[D_x^2 - 1]G(x,x') = \frac{\delta(x-x')}{x}, \tag{17}$$

$$G(0,x') : \text{ finite.} \tag{18}$$

Denoting respectively by $x_<$ and $x_>$ the smaller and larger values of x and x', it is easily verified that

$$G(x,x') = -I_0(x_<)K_0(x_>) + \alpha I_0(x)I_0(x'), \tag{19}$$

where I_0 and K_0 are the modified Bessel functions. The second term on the right hand side reflects the freedom resulting from the absence of a second boundary condition at $x = qR$. We can now repeat the same procedure which led from Eq.(5) to Eq.(10), and later to Eq.(12), with some slight modification due to the presence of the volume element $x\,dx$ in the relevant integrals. Thus we define the operators G and Φ such that their configuration space representations are $\langle x|G|x'\rangle = \sqrt{x}G(x,x')\sqrt{x'}$ and $\langle x|\Phi|x'\rangle = \sqrt{x}\phi(x,x')\sqrt{x'}$. It is not difficult to show that the operator Φ is positive definite, so its square root is well defined. The function $\eta \equiv \Phi^{1/2}x^{1/2}\rho$ then satisfies the integral equation

$$\eta = \mu\Phi^{1/2}(1+G)\Phi^{1/2}\eta, \tag{20}$$

whose kernel is symmetric.

For an annulus with radii $R_1 < R_2$ the Green function has much more freedom because the origin is not reached. Instead of (19) we may now have

$$G(x,x') = -[\alpha I_0(x_<)K_0(x_>) + \beta K_0(x_<)I_0(x_>)] + \gamma I_0(x)I_0(x') + \delta K_0(x)K_0(x'), \tag{21}$$

with $\alpha + \beta = 1$.

We have solved Eqs.(21) numerically for the disk and the annulus geometry using $N = 160$ Gaussian integration points for the radial integration. As a credibility check of our

numerical procedure we have confirmed that the numerical value of the positive eigenvalues is independent of N .

The operator appearing on the right hand side of equation (20) is real and symmetric. One can then look upon the eigenvalue equation as an equation for a rope which is not attached at its ends. This analogy is somewhat expected, since equation (16) is very similar to an inhomogeneous wave equation for stationary solutions. The resulting solutions $\rho_n(x)$ corresponding to positive eigenvalues $\lambda_n = 1/\mu_n$, $n = 0, 1, 2, ..$ with $\lambda_n < \lambda_{n+1}$ appear to have n radial nodes. The lowest mode $n = 0$ cannot satisfy the condition of zero total charge (2), and hence it is physically unacceptable. All the other modes indeed have zero total charge, and can therefore be regarded as representing the pertinent radial charge density.

For the disk geometry we chose $qR = 1$ in Eq.(16) and $\alpha = 0$ in the expression (19) for the Green function. The charge density profile for the lowest four modes $n = 1, 2, 3, 4$ is displayed in Fig. 1. The basic features of these solutions are as follows: 1) The charge density is maximal at the center. 2) The mode $n = 1$ with one zero reminds us of the charge distribution in the Hall bar geometry although it does not have a sharp peak at the edge. 3) Most notably, there are numerous oscillatory solutions which, to the best of our knowledge, were not predicted so far.

For the annulus geometry we chose $qR_1 = 0.5$ and $qR_2 = 1.0$ as integration limits instead of 0 and qR in Eq.(16). We also take $\alpha = 1, \beta = \gamma = \delta = 0$ in the expression (21) for the Green function. The charge density profile for the lowest four modes $n = 1, 2, 3, 4$ is displayed in Fig. 2. The basic features of these solutions are different from the ones found for the disk in that they do not have a maximum at the inner edge. From that point of view, a disk cannot be considered as an annulus with vanishingly small inner radius. The large value of the charge at $R = 0$ is attributed to the weak (but integrable) singularity of $K_0(x)$ near $x = 0$. However, here again there are numerous oscillatory solutions. We know [13] and shall also see in Appendices B and C that in the Hall bar geometry, there is only a single solution, which is monotonic. The novel result of spatial oscillatory charge density must then be related to the fact that the pertinent physical systems are compact. It then belongs

to the realm of mesoscopic and quantum dot physics, which, nowadays, is experimentally accessible.

We now present our results for the current profile in the circular geometry. The derivation of the current once the charge density is given has been explained for the Hall bar geometry in refs. [12,13]. Here we are interested mainly in the oscillatory pattern. It is not difficult to show that the tangential current $J_\theta(x = qr)$ is given by,

$$J_\theta(x) = a\frac{1}{x}\int_{qR_1}^{x} x'\rho(x')dx' + b, \tag{22}$$

where a and b are constants and $R_1 = 0$ for the disk and finite for the annulus. In the following we display the integral appearing on the RHS of (22) since it gives the main characteristics of the actual current. In figure 3 the current profile for the disk is shown, for the same configuration as in figure 1. The current of the lowest mode is similar in shape to the current evaluated in the Hall bar geometry [1,13]. The current of other modes is oscillating, which shows clearly that for these modes, current is not concentrated solely near the edges. Similar result occurs also for the annulus geometry, for which the current of the four modes pertinent to figure 2 is displayed in figure 4.

One of us (Y.A) would like to thank the Japanese Society for the Promotion of Science for supporting his visit to the Institute for Solid State Physics in which this work has been carried out.

APPENDIX A

Solution of the equation for the integer QHE.

In this appendix we present a Green function solution of the equations derived in Ref. [1] for the integer quantum Hall effect in a Hall bar. If the Hall bar stretches along the y direction between points $x = L_1$ and $x = L_2$, the charge density and the electrostatic potential depend only on x. They are determined by a set of equations,

$$V(x) = -2e^2 \int_{L_1}^{L_2} \log|x - x'|\rho(x')dx' \tag{23}$$

$$\rho(x) = \frac{n}{h\omega_c} V''(x), \tag{24}$$

where n is the Landau level number and ω_c is the cyclotron frequency. Transforming to dimensionless coordinates $x \to qx$ this set of equations is equivalent to a single equation for $\rho(x)$ which, for antisymmetric solutions reads

$$-\rho(x) = \mu \frac{d^2}{dx^2} \int_0^{qL_x} \log\left|\frac{x - x'}{x + x'}\right| \rho(x')dx', \tag{25}$$

where $\mu \equiv (4e^2nq)/(h\omega_c) > 0$ and $L_x = L_2 = -L_1$ is half the width of the Hall bar. Here q is just a parameter with dimensions of inverse length. In order to apply our Green function method for solving Eq.(25) we add ρ'' on both sides and use algebraic manipulations as in Section 2. The result, using the notation of section 2, is

$$-G\rho = \mu(1 + G)L\rho. \tag{26}$$

If we apply the operator $(1 + G)^{-1}$ on both sides, we get

$$[1 - (1 + G)^{-1}]\rho = \mu(-L)\rho. \tag{27}$$

Equation (27) is of the form (4) with symmetric A and symmetric positive definite B and therefore it has real eigenvalues μ. It would have been more useful to solve an equation for the potential $V(x)$ rather than the density $\rho(x)$, since the later one is known to have a power singularity near the edges [1,2,13]. Unfortunately we were unable to obtain an equation of the form (4) with symmetric A and symmetric positive definite B.

The charge density in a Hall bar for the integer QHE is displayed in Fig. 5. For the actual numerical solution we take the Hall bar to be located between $x = -2$ and $x = +2$ in order to compare the charge density of the non-interacting system with that of the interacting system reported below in Appendix B. As can convincingly be inferred from Fig. 5 the charge density in the integer quantum Hall regime is singular near the edge. This is of course consistent with earlier results [1,2,13].

APPENDIX B

Charge density profile in the Hall bar geometry for the fractional QHE.

As was stated already, the charge distribution profile in the Hall bar geometry for the fractional quantum Hall system was calculated by an analytic iterative method [13]. In this appendix we present the exact solution obtained within the Green function technique introduced in Section 2. We have solved Eq.(12) numerically using mesh of $N = 400$ integration points between 0 and 2, replacing the operators by $N \times N$ matrices. The weak logarithmic singularity at $x = x'$ is of course integrable. Out of the N eigenvalues only one is found to be positive. This feature as well as the numerical value of the positive eigenvalue persist independent on the number N (provided it is sufficiently large). The parameters qL (upper limit of integration in Eq.(10) and α (the free parameter in the Green function (8) should be chosen in such a way that Eq.(12) has at least one positive eigenvalue. In all our attempts, we could not obtain more than a single positive eigenvalue, a result which is markedly distinct from that obtained in the circular geometry. For the special choice $qL = 2$ and $\alpha = 0$ the charge density in a Hall bar is displayed in Fig. 6. It is reassuring to note that this solution is extremely close to the one obtained by iteration methods [13] or the one obtained by solving Eq.(12) using a power basis technique as explained in the next Appendix.

APPENDIX C

Solution of the equations in the Hall bar using a power series expansion.

In this appendix we present an alternative formulation to study the integro-differential Eq.(3) in the form

$$u(x) - au''(x) = -\mu \int_{-1}^{1} dx' \ln|x - x'| u''(x'), \tag{28}$$

with the antisymmetry condition $u(-x) = -u(x)$. Here, we have used the notation $\rho(x) = u''(x)$. We can then choose $\{x^{2k+1} | k = 0, 1, \cdots\}$ as an expansion basis. The integration

operator on the RHS of (28) is represented as

$$\begin{aligned} L \cdot x^{2l+1} &= -\int_{-1}^{1} dx' \ln|x-x'| x'^{2l+1} \\ &= \sum_{k=0}^{\infty} \frac{-2}{(2k+1)(2k-2l-1)} x^{2k+1}, \end{aligned} \tag{29}$$

whose matrix representation reads

$$L = \begin{pmatrix} 2 & \frac{2}{3} & \frac{2}{5} & \frac{2}{7} & \cdots \\ -\frac{2}{3} & \frac{2}{3} & \frac{2}{9} & \frac{2}{15} & \\ -\frac{2}{15} & -\frac{2}{5} & \frac{2}{5} & \frac{2}{15} & \\ -\frac{2}{35} & -\frac{2}{21} & -\frac{2}{7} & \frac{2}{7} & \\ \vdots & & & & \ddots \end{pmatrix}, \tag{30}$$

and the double derivative is

$$D^2 x^{2l+1} = \frac{d^2}{dx^2} x^{2l+1} = (2l+1)(2l) x^{2l-1}.$$

Thus we have

$$(1 - aD^2)u = \mu L D^2 u.$$

Since the double derivative D^2 has rapidly increasing next-diagonal elements $(2l+1)(2l)$, it seems impossible to simulate the eigenvalue problem (28) numerically with any finite size truncation of D^2. A remedy for this is to integrate twice the original equation (28). Let us introduce the double integration operator I^2 by

$$I^2 x^{2l+1} = c_l x + \frac{1}{(2l+3)(2l+2)} x^{2l+3},$$

where c_l is an integration constant. Then all the solutions of equation

$$I^2 (I^2 L)^{-1} (I^2 - a) u = \mu u,$$

also satisfy equation (28). After finding some suitable set of constants c_l, we obtain a positive eigenvalue μ whose eigenvector is consistent with the one obtained by the Green function method and by an analytic argument [13].

REFERENCES

[1] A. H. Macdonald, M. Rice and D. Brinkman, Phys. Rev. B**28**, 3648 (1983).

[2] D. J. Thouless, J. Phys. C **18**, 6211 (1985).

[3] S. Kivelson, D.- H.Lee and S.-C. Zhang, Phys. Rev. B **46**, 2223 (1992).

[4] S.C. Zhang, T.H. Hansson, and S. Kivelson, Phys. Rev. Lett. **62**, 82 (1989); S.C. Zhang, Int. J. Mod. Phys. B**6**, 25 (1992) and references therein; A. Zee, in *Field Theory, Topology and Condensed Matter Physics*,Proceedings of the Ninth Chris Engelgrecht Summer School in Theoretical Physics, ed. H.B. Geyer, (Springer-Verlag Berlin Heidelberg, 1995) and references therein.

[5] C. Wexler and D. J. Thouless, Phys. Rev. B **49**, 4815 (1994).

[6] J. Dempsey, B. Y. Gelfand and B. I. Halperin, Phys. Rev. Lett. **70**, 3639 (1993).

[7] D. B. Chklovskii, B. I. Shklovskii and L.I. Glazman, Phys.Rev. B **46**, 4026 (1992); D. Pfannkuche and J. Hajdu, Phys.Rev. B **46**, 7032 (1992); D. B. Chklovskii, K. A. Matveev and B. I. Shklovskii, Phys.Rev. B **47**, 12605 (1993); L. Brey, J. J. Palacios and C. Tejedor, Phys.Rev. B **47**, 13884 (1993).

[8] X. G. Wen, Phys. Rev. B**40**, 7387 (1989); Int. J. Mod. Phys. B**2**, 239 (1990).

[9] D. Orgad and S. Levit, Phys. Rev. Lett. **77**, 719 (1996); D. Orgad, Phys. Rev. Lett. **79**, 475 (1997).

[10] J. H. Han, *Green's Function Approach to the Edge Spectral Density*, cond-mat/9702074.

[11] M. P. A. Fisher and L. I. Glazman, *Transport in a one-dimensional Luttinger liquid*, to appear in Mesoscopic Electron Transport.

[12] N. Nagaossa and M. Kohmoto, Phys. Rev. Lett. **75**, 4294 (1995).

[13] J. Shiraishi and M. Kohmoto, Phys. Rev. B**54**, 17667 (1996).

FIGURES

FIG. 1. Charge distribution in a disk. The parameters are $qR = 1$ and $\alpha = 0$ (see equation (19)). The four modes correspond to the four positive eigenvalues $\lambda_n \equiv 1/\mu_n$ of equation (20), with $n = 1, 2, 3, 4$ which also counts the number of radial nodes.

FIG. 2. Charge distribution in an annulus. The parameters are $qR_1 = 0.5$, $qR_2 = 1$ and $\alpha = 1$, $\beta = \gamma = \delta = 0$ (see equation (21)). The four modes are as in figure 1.

FIG. 3. Current distribution in a disk. The parameters are $qR = 1$ and $\alpha = 0$ (see equation (19)). The four modes correspond to the four positive eigenvalues $\lambda_n \equiv 1/\mu_n$ of equation (20), with $n = 1, 2, 3, 4$ which also counts the number of radial nodes.

FIG. 4. Current distribution in an annulus. The parameters are $qR_1 = 0.5$, $qR_2 = 1$ and $\alpha = 1$, $\beta = \gamma = \delta = 0$ (see equation (21)). The four modes are as in figure 3.

FIG. 5. Charge distribution in a Hall bar for the integer quantum Hall system obtained by solving equation (27). The Hall bar is located between $x = -2$ and $x = 2$ and the charge distribution is antisymmetric. The parameter α in the Green function (8) is set equal to zero.

FIG. 6. Charge distribution in a Hall bar for the fractional quantum Hall system obtained by solving equation (12). The Hall bar is located between $x = -2$ and $x = 2$ and the charge distribution is antisymmetric. The parameter α in the Green function (8) is set equal to zero.

Fig.5

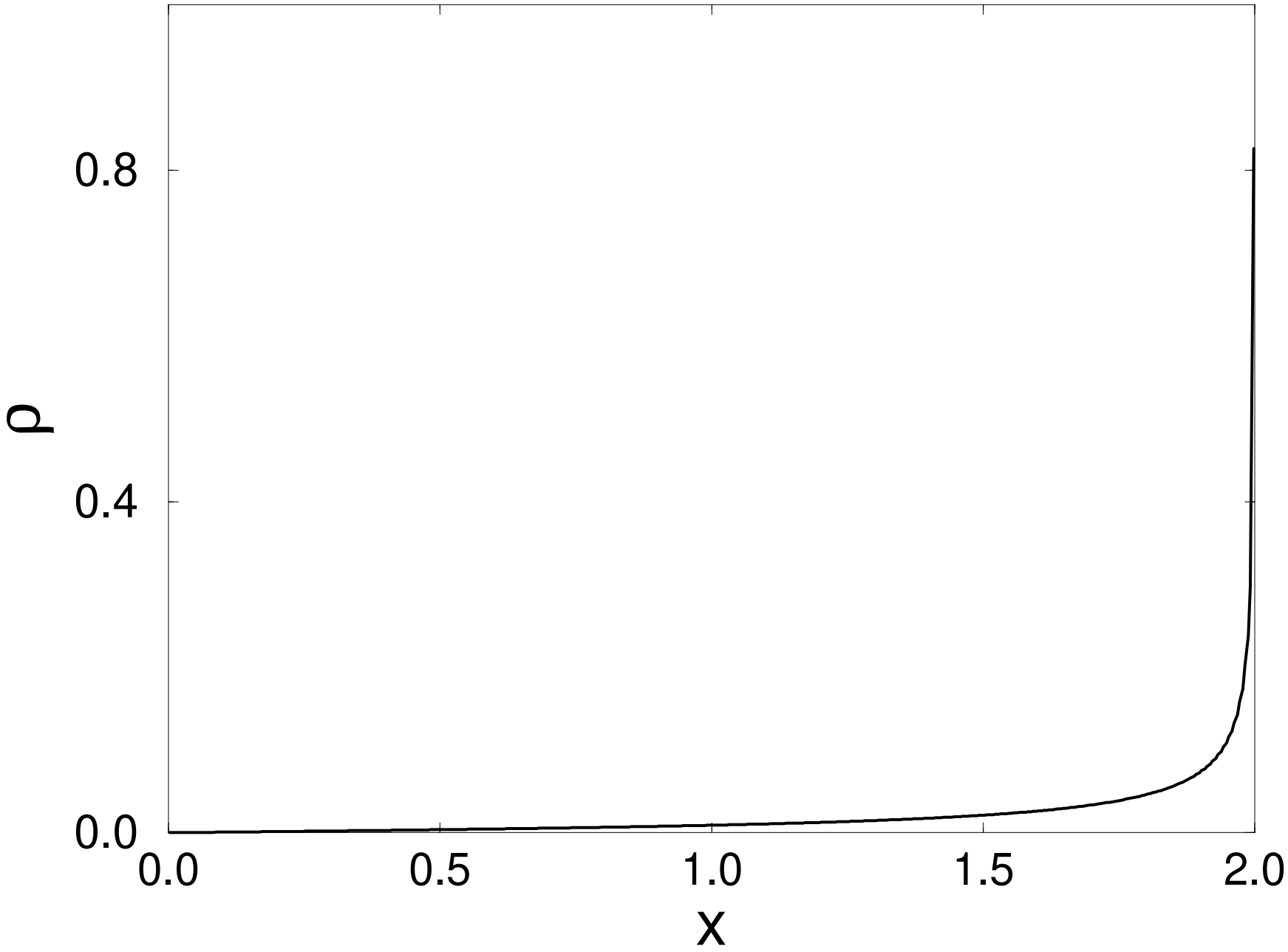

Fig.2

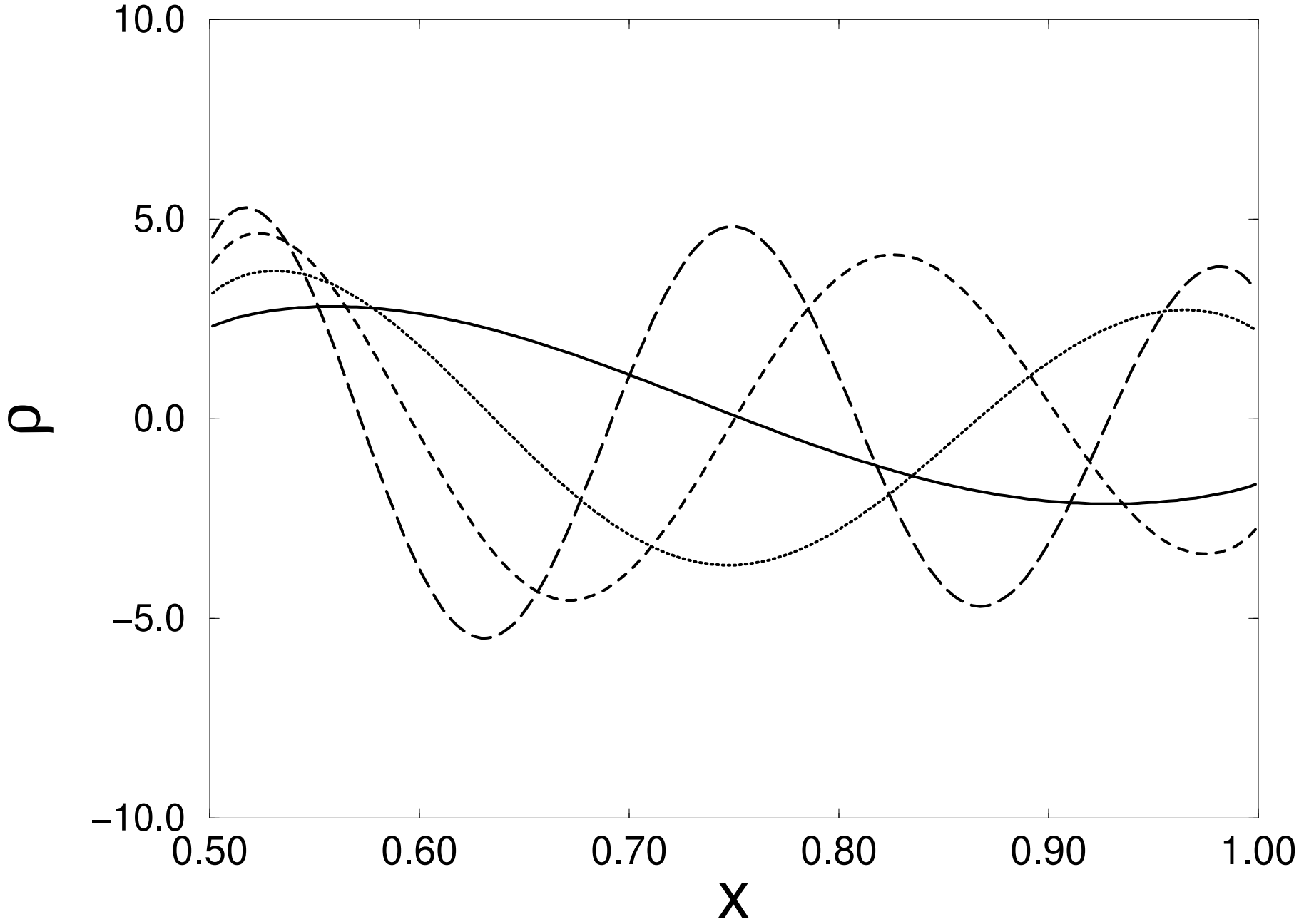

Fig.6

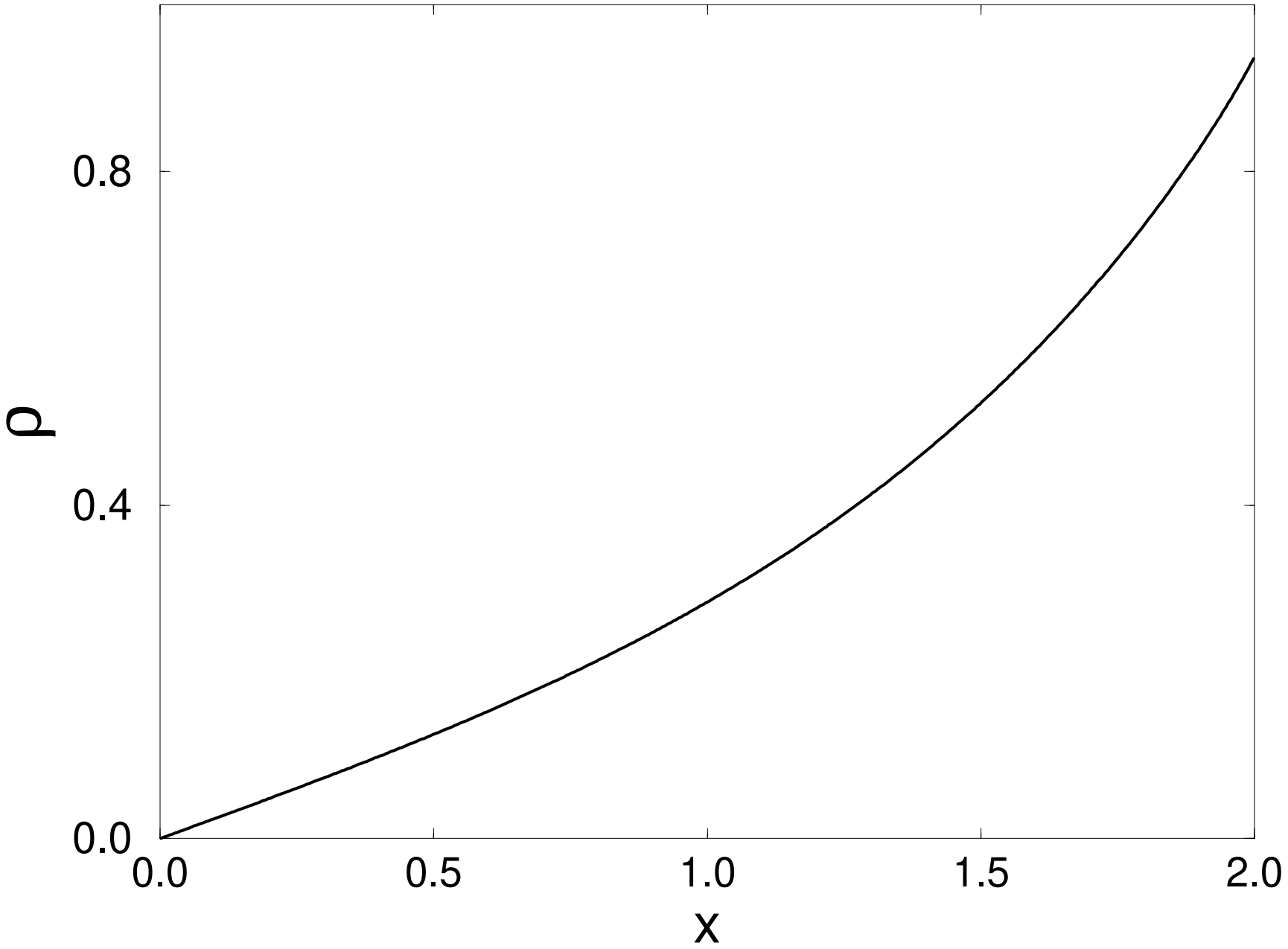

Fig.4

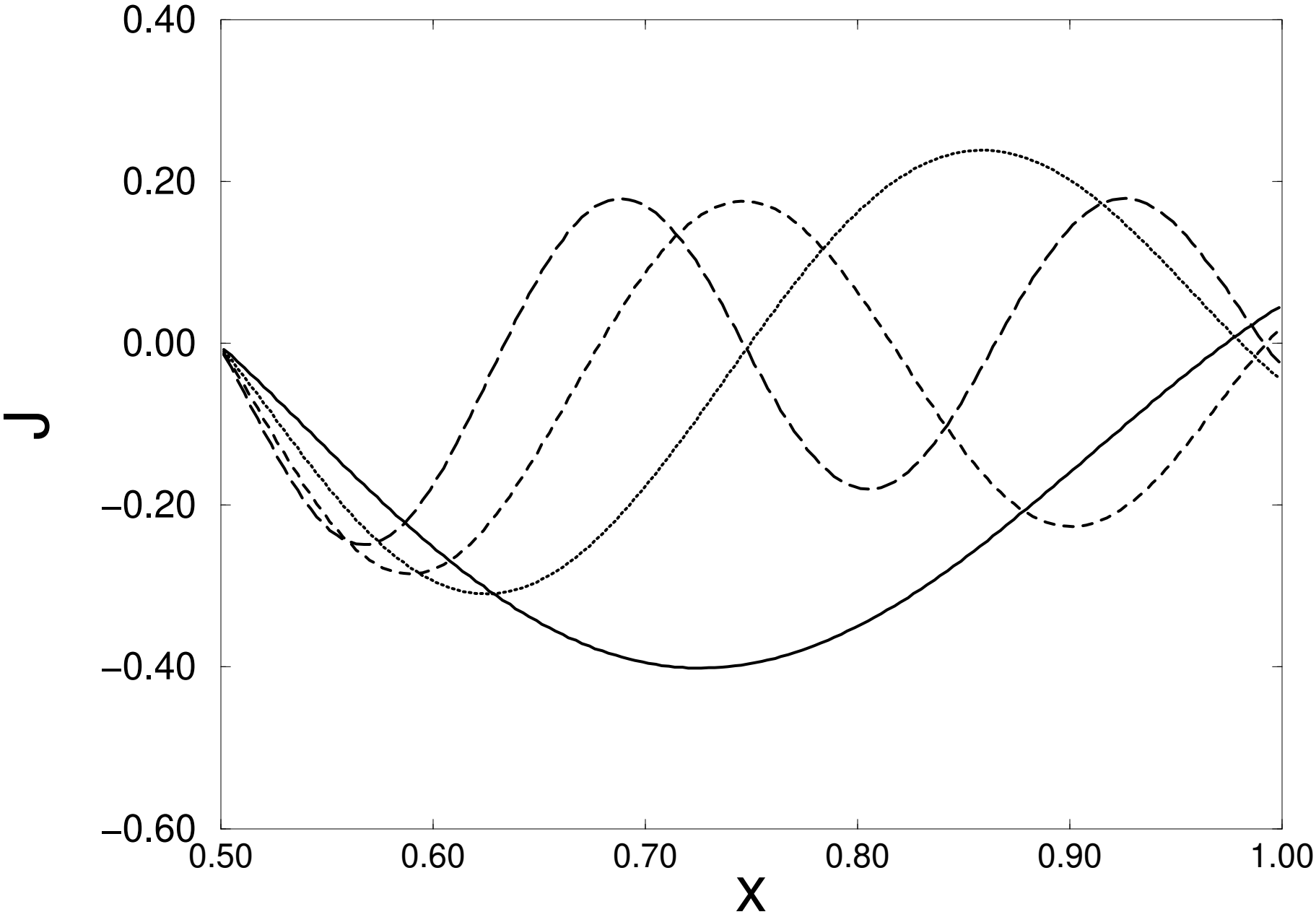

Fig.3

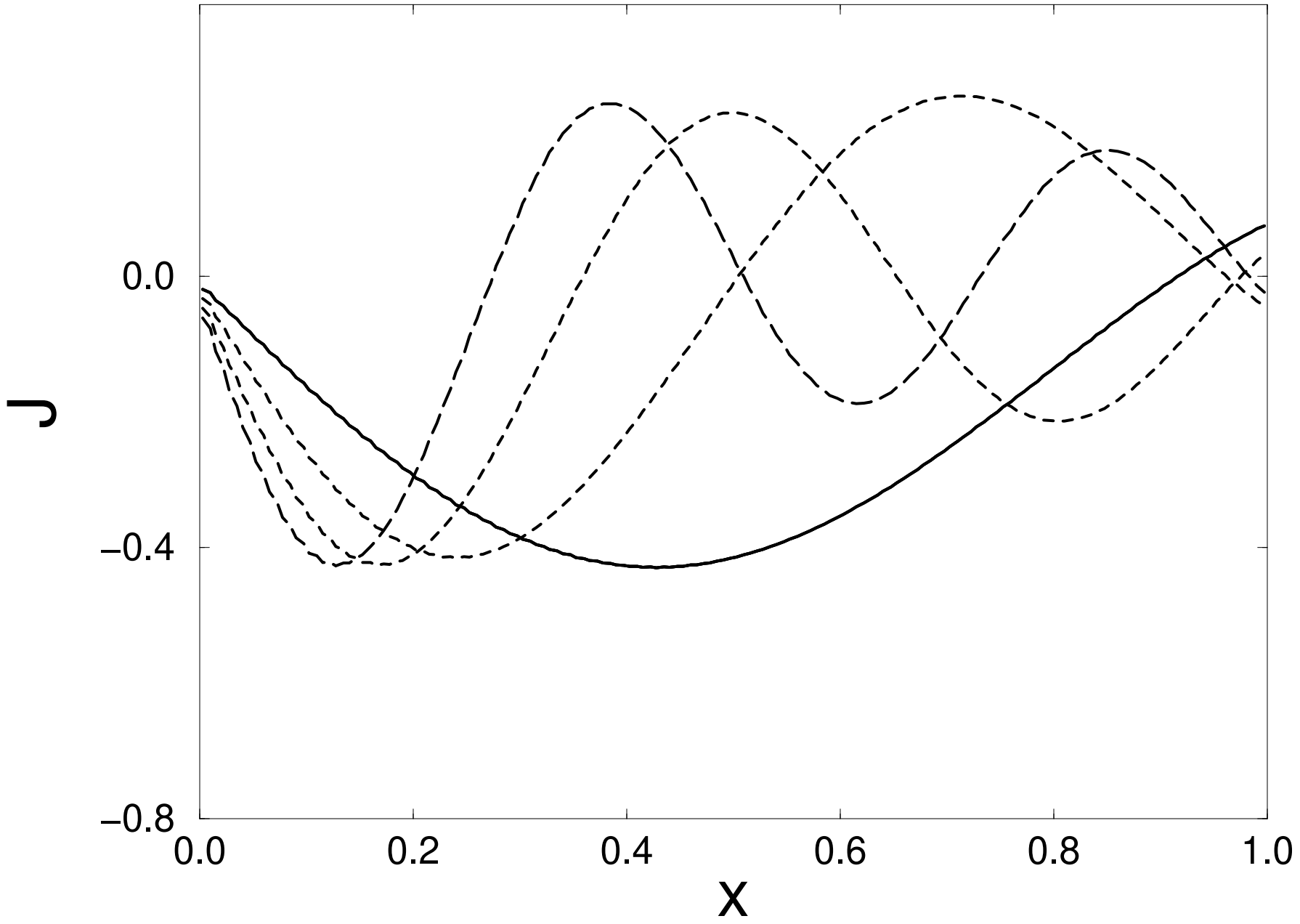

Fig.1